Derivation and analysis of a fluid-dynamical model in thin and long elastic vessels

Debora Amadori * Stefania Ferrari † Luca Formaggia†

Abstract

Starting from the three-dimensional Newtonian and incompressible Navier-Stokes equations in a compliant straight vessel, we derive a reduced one-dimensional model by an averaging procedure which takes into consideration the elastic properties of the wall structure. In particular, we neglect terms of the first order with respect to the ratio between the vessel radius and length. Furthermore, we consider that the viscous effects are negligible with respect to the propagative phenomena. The result is a one-dimensional nonlinear hyperbolic system of two equations in one space dimension, which describes the mean longitudinal velocity of the flow and the radial wall displacement. The modelling technique here applied to straight cylindrical vessels may be generalized to account for curvature and torsion.

An analysis of well posedness is presented which demonstrates, under reasonable hypothesis, the global in time existence of regular solutions.

Introduction

The use of reduced models to study the fluid-structure interaction in compliant vessels is rather well established. Typical applications range from the haemodynamics of large arteries to the investigation of hammer effects in hydraulic networks. These models are quite accurate in the description of the wave propagation phenomena typical of this type of problems and are much cheaper in terms of computational cost compared to a full three-dimensional model.

AMS Subject Classification: 76Z05, 35Q30, 74F10, 35L50

*Dip. di Matematica Pura e Applicata, Università degli Studi dell'Aquila.

†MOX, Dipartimento di Matematica, Politecnico di Milano.

An increased interest in these models in the context of haemodynamic applications has been driven by the "geometrical multiscale approach" for simulating the mutual interaction between local and systemic dynamics (see [8],[9],[10]). In this frame, reduced models play the role of representing the global behavior of the circulatory system or large parts of it, which interact with local descriptions made by means of more sophisticated models. One-dimensional models are here of interest because of their capability of accurately represent pulse waves in large arteries (see [15],[19]).

Simplifying assumptions are usually necessary for their derivation. In particular, it is assumed that the flow is mainly in the axial direction and that the effects of the viscosity are negligible with respect to the propagative effects under study. Indeed the viscous terms are either completely neglected, as in [19], or accounted for by a source term, as in [14] and [2]. Here, we use this hypothesis in the set up of the fluid-structure interface condition, where we do not explicitly enforce a no-slip condition. Moreover we suppose that the profile of the axial component of the velocity is such that the non-linear advective term in the momentum equation can be suitably treated. Under these hypotheses we are able to derive a system of just two equations that describe the evolution of mean flux and pressure. With respect to the derivation of similar model, we have here avoided to make any assumption that could impede to generalize the model to curved vessels. Therefore, even if the results here presented are specialized for straight vessels, the derivation can be generalized to a different metric. Work is indeed ongoing in this direction and this extension will be the subject of a forthcoming paper.

We mention that in [3] a different one-dimensional model for compliant vessels is advocated, which does not require any closure assumption on the longitudinal velocity profile. The authors show that the model is accurate to the second order with respect to the ratio between the vessel radius length scales. However, this model requires to solve an additional equation and its complexity reduces its applicability in practice.

The role of longitudinal displacements of the vessel wall has been recently pointed out in [5]. This work shows their small relative importance for haemodynamic applications, which are the main concern of the present work. Therefore we have chosen to describe the vessel wall in terms of a linear elastic and axi-symmetric structure which allows only radial displacements. Differently from previous works we will not use a shell type representation of the structure as we preferred to derive the law governing the structure dynamics directly from the Navier

equation, through some simplifying assumptions. By our asymptotic analysis we finally obtain an algebraic law linking the pressure to the measure of the vessel section, which is constant on each cross-section as in [2]. The resulting expression is indeed similar to that obtained for membrane shells, with a correction term that accounts for moderately thick walls. This algebraic law can be used as a closing relation for our one dimensional model.

The way of reducing the three-dimensional Navier-Stokes system and of handling the boundary conditions proposed in the present article, has been inspired by the derivation of the equations for shallow water flow introduced in [13] and later refined in [6] and in [7]. In particular we consider three dynamic boundary conditions prescribing the equilibrium of the stresses at the fluid-structure interface and one kinematic condition which guarantees the continuity of the radial velocity at the fluid-structure interface. On the other hand, in [14] and [2] authors force the longitudinal and the circumferential components of the velocity to vanish at the fluid-structure interface and they impose continuity of the radial velocity; they take only the radial component of the dynamic equilibrium equations into account.

The more common one-dimensional models present in the literature, and our model as well, are given by hyperbolic systems of two differential equations in one space dimension. In [2] a rather complete mathematical analysis is carried out in the space-time half-plane. In particular they analyze the blow-up of regular solutions due to the non linear effects in the case that the system is homogeneous with no source term. They find that, being the typical vessel length of an artery much shorter than the space required for a discontinuity to develop, the wave propagation in the arterial system may considered of regular type. In this paper we present a general well posedness analysis and prove the global in time existence of regular solutions on a bounded spatial domain, in the case of constant coefficients and no source term and when either the pressure or the velocity are prescribed at the inlet and a non-reflecting boundary condition is used at the outlet. Given bounds on the C^0-norm of the initial and boundary data and sufficiently smallness of their derivatives are also required. The result has been obtained by extending and specializing the results on semi-global in time existence of smooth solution proposed in [18]. The analysis may be applied to a wide class of one-dimensional models. We have then assessed our model with numerical tests.

The outline of this paper is as follows. In the Section 1 we introduce the three-dimensional fluid-structure interaction model we are moving from and the rescaling of the system needed for

the successive derivations. In the Section 2 we derive the one-dimensional system by averaging the rescaled model. In the Section 3, we provide a complete mathematical analysis; in particular we prove a global in time existence and uniqueness result for smooth solutions on a finite space-domain. In the Section 4 we provide some numerical experiments in order to validate our new model and compare it with the model previously proposed in [14]. Some conclusions are drawn in Section 5 and some details on the geometrical framework we are dealing with are collected in the Appendix at the end of the paper.

1 The 3D fluid-structure-interaction model

In this section we detail the fluid and the vessel wall dynamics in cylindrical coordinates in their respective space-time domains. We describe the wall dynamics through a linear elastic and isotropic stress-strain law as in [11]. We also consider only radial displacements. Furthermore, we will assume that the shear component of the Cauchy stresses in the wall are negligible once the equations are written in the natural coordinate frame of the vessel wall.

The imposition of the continuity of the radial velocity and of the stresses at the fluid-structure interface completes the setting of the 3D fluid-structure interaction model. We will not enforce the continuity of the axial and circumferential components of the velocity at the interface explicitly.

Finally, by introducing a suitable rescaling of the whole model we approximate the equations to the first order with respect to the ratio between the vessel radius and length and derive a first-order approximate expression for the pressure of the fluid.

1.1 The fluid-dynamics

The time-dependent fluid domain and its boundaries. Let $L > 0$ be the total length of an axi-symmetric vessel with circular cross-section, let $T > 0$ be the total evolution time and let

$$\eta : [0, T] \times [0, L] \to \mathbb{R}^+, \qquad \eta_0 : [0, L] \to \mathbb{R}^+ \tag{1.1}$$

be the radial distance of the fluid-wall interface from the centerline (see Fig. 1), during the motion and in the reference configuration, respectively. We are here assuming that the vessel wall allows only radial displacements. The space domain we are dealing with may be described

in cylindrical coordinates, using the notation

$$x^1 = r, \quad x^2 = \theta, \quad x^3 = z, \tag{1.2}$$

where z is aligned along the vessel axis, assumed fixed. We refer to [1] for a reminder of vector analysis in the cylindrical coordinate system.

At any $t \in [0, T]$ the fluid domain is given by

$$\mathcal{U} = \{(r, \theta, z) \in [0, \eta(t, z)) \times [0, 2\pi) \times (0, L)\}. \tag{1.3}$$

Its boundary is split into three different parts: the inlet $\mathcal{L}_{in}$, the outlet $\mathcal{L}_{out}$ and the vessel wall interface $\mathcal{S}$ (see Fig. 1)[1]. We have, for $t \in [0, T]$

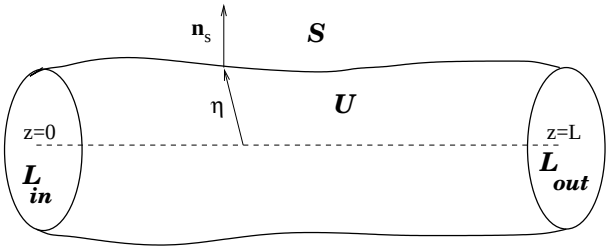

Figure 1: The time-dependent axi-symmetric domain $\mathcal{U}$ and its boundary at a given time t

$$\begin{aligned} \mathcal{L}_{in} &= \{(r, \theta, 0) : (r, \theta) \in [0, \eta(t, 0)) \times [0, 2\pi)\}, \\ \mathcal{L}_{out} &= \{(r, \theta, L) : (r, \theta) \in [0, \eta(t, L)) \times [0, 2\pi)\}. \end{aligned} \tag{1.4}$$

while

$$\mathcal{S} = \{(\eta(t, z), \theta, z) : (\theta, z) \in [0, 2\pi) \times (0, L)\}, \quad t \in [0, T]. \tag{1.5}$$

We will indicate the outward radial normal to $\mathcal{S}$ by $\boldsymbol{n}_{\mathcal{S}}$. It may be readily verified that its coordinates are given in physical components by

$$\boldsymbol{n}_{\mathcal{S}} = c_s \left(1, 0, -\frac{\partial \eta}{\partial z}\right) \quad \text{with } c_s = \left[1 + \left(\frac{\partial \eta}{\partial z}\right)^2\right]^{-1/2}. \tag{1.6}$$

From now on we will adopt the summation convention and, whenever not otherwise indicated, repeated indices i, j, k, l run from 1 to 3. Furthermore, we will indicate the physical components of a tensor B in cylindrical coordinates either as $B(ij)$ or, alternatively, as B_{rr}, $B_{r\theta}$ etc.

[1] In haemodynamic applications the terms proximal and distal are usually referred to as inlet and outlet, respectively

The Navier-Stokes equations The physical components of the rate of deformation tensor D in (physical) cylindrical coordinates are

$$D_{rr} = \frac{\partial u_r}{\partial r}, \quad D_{\theta\theta} = \frac{1}{r}\frac{\partial u_\theta}{\partial \theta} + \frac{u_r}{r}, \quad D_{zz} = \frac{\partial u_z}{\partial z}, \quad D_{rz} = \frac{1}{2}\left(\frac{\partial u_r}{\partial z} + \frac{\partial u_z}{\partial r}\right), \tag{1.7}$$
$$D_{r\theta} = \frac{1}{2}\left(r\frac{\partial}{\partial r}\left(\frac{u_\theta}{r}\right) + \frac{1}{r}\frac{\partial u_r}{\partial \theta}\right), \quad D_{z\theta} = \frac{1}{2}\left(\frac{1}{r}\frac{\partial u_z}{\partial \theta} + \frac{\partial u_\theta}{\partial z}\right).$$

while the components of the Cauchy stress tensor T_N for a Newtonian fluid are given by

$$T_N(ij) = -P\delta^{ij} + \hat{\sigma}(ij), \tag{1.8}$$

being P the pressure, δ^{ij} the Kronecker symbol and $\hat{\sigma}(ij) = 2\hat{\mu}D(ij)$, where $\hat{\mu}$ is the viscosity of the fluid. It is a common practice to divide the momentum equation by the constant density. We will therefore indicate

$$\frac{T_N(ij)}{\varrho} = -p\delta^{ij} + \sigma(ij) \tag{1.9}$$

where $\sigma(ij) = 2\mu D(ij)$; μ is here the kinematic viscosity and p is the pressure scaled by the fluid density. Finally, the Navier-Stokes equations in cylindrical coordinates may be written as

$$\begin{cases} \dfrac{\partial}{\partial r}(ru_r) + \dfrac{\partial u_\theta}{\partial \theta} + \dfrac{\partial}{\partial z}(ru_z) = 0, \\ \dfrac{\partial u_r}{\partial t} + \dfrac{1}{r}\dfrac{\partial\left(ru_r^2\right)}{\partial r} + \dfrac{1}{r}\dfrac{\partial\left(u_r u_\theta\right)}{\partial \theta} + \dfrac{\partial(u_r u_z)}{\partial z} - \dfrac{1}{r}u_\theta^2 = \\ \qquad -\dfrac{\partial p}{\partial r} + \dfrac{1}{r}\dfrac{\partial\left(r\sigma_{rr}\right)}{\partial r} + \dfrac{1}{r}\dfrac{\partial \sigma_{r\theta}}{\partial \theta} + \dfrac{\partial \sigma_{rz}}{\partial z} - \dfrac{\sigma_{\theta\theta}}{r}, \\ \dfrac{\partial u_\theta}{\partial t} + \dfrac{\partial(u_r u_\theta)}{\partial r} + \dfrac{1}{r}\dfrac{\partial(u_\theta^2)}{\partial \theta} + \dfrac{\partial(u_\theta u_z)}{\partial z} + \dfrac{2}{r}u_\theta u_r = \\ \qquad -\dfrac{1}{r}\dfrac{\partial p}{\partial \theta} + \dfrac{\partial \sigma_{r\theta}}{\partial r} + \dfrac{1}{r}\dfrac{\partial \sigma_{\theta\theta}}{\partial \theta} + \dfrac{\partial \sigma_{\theta z}}{\partial z} + \dfrac{2}{r}\sigma_{r\theta}, \\ \dfrac{\partial u_z}{\partial t} + \dfrac{1}{r}\dfrac{\partial(ru_r u_z)}{\partial r} + \dfrac{1}{r}\dfrac{\partial(u_z u_\theta)}{\partial \theta} + \dfrac{1}{r}\dfrac{\partial\left(ru_z^2\right)}{\partial z} = \\ \qquad -\dfrac{\partial p}{\partial z} + \dfrac{1}{r}\dfrac{\partial(r\sigma_{rz})}{\partial r} + \dfrac{1}{r}\dfrac{\partial \sigma_{z\theta}}{\partial \theta} + \dfrac{1}{r}\dfrac{\partial\left(r\sigma_{zz}\right)}{\partial z}. \end{cases} \tag{1.10}$$

1.2 The dynamics of the vessel wall

We will here consider the equations necessary to account for the wall compliance. Following the route usually taken to derive reduced models we will assume that the wall inertia is negligible,

that is the wall is instantaneously in equilibrium. The configuration at time t of the vessel wall is given by:

$$\mathcal{W} = \{(r, \theta, z) : (\theta, z) \in [0, 2\pi) \times (0, L), r \in [\eta(t, z), \eta(t, z) + k(t, z)]\} \tag{1.11}$$

where $k = k(t, z) > 0$ indicates the thickness of the wall. The inner part of the vessel wall coincides with the fluid-structure interface $\mathcal{S}$ introduced in (1.5) (see Figure 2); more precisely $\mathcal{W}_{|r=\eta} = \mathcal{S}$. The current and the reference position of a point of the wall is given respectively by:

$$\boldsymbol{w} : (0, T) \times \mathcal{W} \to \mathbb{R}^3, \quad \boldsymbol{w}_0 : \mathcal{W} \to \mathbb{R}^3$$

where $\boldsymbol{w}$ depends on the dynamics of the wall, while $\boldsymbol{w}_0$ is a known function. For a complete description of function $\boldsymbol{w}$ see (A.3) in the Appendix. On the wall it is also possible to identify a different coordinate system, (s, θ, l), aligned with the current configuration. Its definition is detailed in the Appendix as well. Since we are considering only radial displacements, we may write

$$w_\theta = w_{0\theta}, \quad w_z = w_{0z}. \tag{1.12}$$

Furthermore, we have the following identities

$$\eta(t, z) = w_r(t, \eta(t, z), \theta, z), \quad \eta_0(z) = w_{0r}(\eta_0(z), \theta, z), \quad (t, \theta, z) \in (0, T) \times (0, 2\pi] \times (0, L)\,.$$

Let ψ^i be the 1-contravariant displacement vector given by

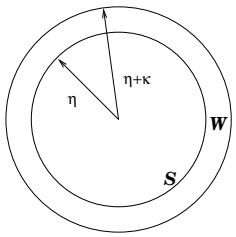

Figure 2: The time-dependent axisymmetric domain $\mathcal{W}$

$$\psi^1 = w_r - w_{0r}, \quad \psi^2 = w_\theta - w_{0\theta} = 0, \quad \psi^3 = w_z - w_{0z} = 0.$$

The general formulation of the infinitesimal strain tensor in 2-covariant form (see [11]) is

$$e_{ij} = \frac{1}{2}\left(\psi_{i,|j} + \psi_{j,|i}\right) = \frac{1}{2}\left(\frac{\partial \psi_i}{\partial x^j} + \frac{\partial \psi_j}{\partial x^i}\right) - \Gamma^l_{ij}\psi_l \tag{1.13}$$

where Γ^l_{ij} are the Christoffel symbols connected to the orthogonal metric (A.5). The familiar linear elastic relation that provides the Cauchy stress tensor is given by

$$T_{ij} = 2Ge_{ij} + \lambda e_{kk} g_{ij} \tag{1.14}$$

and, in physical components,

$$T(ij) = 2Ge(ij) + \lambda e_{kk}\delta_{ij} \tag{1.15}$$

where G and λ are, in general, functions of z. It is worth recalling the usual relationships

$$G = \frac{E}{2(1+\xi)}\,, \qquad \lambda = \frac{\xi E}{(1-2\xi)(1+\xi)} \tag{1.16}$$

where $E \geq 0$ is the Young modulus and $\xi \in (0, 1/2)$ the Poisson ratio. We will consider the following hypotheses:

1. The thickness of the vessel is uniform, that is $k(t, z) = k_0$ and is small in comparison with the radius of the vessel.

2. As a consequence of the previous assumption we consider that $e_{\theta\theta}$ is constant across the thickness of the vessel wall. In particular we will set $e_{\theta\theta} = \frac{\eta - \eta_0}{\eta}$.

3. The Cauchy stress tensor is aligned with the local reference frame $\boldsymbol{t}$, $\boldsymbol{n}$, $\boldsymbol{b}$ (see the Appendix). That is, in this reference frame shears are negligible (see [12]). This assumption derives from the fact that the fibers that form the structural part of the wall of a blood vessel are approximately aligned with the local frame and show little resistance to bending. As a consequence, the Cauchy stress tensor in the local reference frame, here indicated by $\mathcal{T}$, is assumed to be diagonal.

4. We neglect the inertial effects in the wall structure, that is the wall structure is always in static equilibrium.

5. We finally assume that the pressure external to the vessel is zero. This is not a restrictive hypothesis since the isotropic contribution of the external pressure may be added a-posteriori.

Exploiting (1.15) and recalling the usual relationship between the traces $\mathcal{T}_{kk} = (2G + \lambda)e_{kk}$ and assumption 3, we can express the components of the (diagonal) elastic stress tensor $\mathcal{T}$ in

the local reference frame $\mathbf{t}$, $\mathbf{n}$, $\mathbf{b}$ as

$$\begin{cases} \mathcal{T}_{\theta\theta}(\eta) = 2G\frac{\eta-\eta_0}{\eta} + \frac{\xi}{1+\xi}(\mathcal{T}_{ss}(\eta) + \mathcal{T}_{\theta\theta}(\eta) + \mathcal{T}_{ll}(\eta)) \\ \mathcal{T}_{ll}(\eta) = \frac{\xi}{1+\xi}(\mathcal{T}_{ss}(\eta) + \mathcal{T}_{\theta\theta}(\eta) + \mathcal{T}_{ll}(\eta)), \end{cases} \tag{1.17}$$

on the fluid structure interface $r = \eta$. In order to close the system we evaluate $\mathcal{T}_{ss}(\eta)$ by solving the equation of static equilibrium along the direction $\mathbf{n}$. By using the symbols s, θ and l to denote the physical components, as described in the Appendix, the equilibrium in the s direction gives

$$0 = [\mathbf{div}(\mathcal{T})]_s = \frac{1}{h_\theta h_l}\frac{\partial}{\partial s}\left(\frac{h_\theta h_l}{h_s}\mathcal{T}_{ss}\right) + \frac{1}{h_s}\Gamma^s_{ss}\mathcal{T}_{ss} + \frac{h_s}{h_\theta^2}\Gamma^s_{\theta\theta}\mathcal{T}_{\theta\theta} + \frac{h_s}{h_l^2}\Gamma^s_{ll}\mathcal{T}_{ll}. \tag{1.18}$$

In our case

$$h_s = 1, \quad h_\theta = r = \eta + s\cos\psi, \quad h_l = 1 + s\chi,$$

and

$$\Gamma^s_{ss} = 0 \quad \Gamma^s_{\theta\theta} = -r\cos\psi \quad \Gamma^s_{ll} = -\chi(1+s\chi),$$

where the quantities $\cos\psi$ and χ depend on the geometry and are defined in (A.4). Therefore, (1.18) gives

$$\frac{1}{r}\left[\frac{\partial}{\partial s}\left(r(1+s\chi)\mathcal{T}_{ss}\right) - \cos\psi(1+s\chi)\mathcal{T}_{\theta\theta}\right] - \chi\mathcal{T}_{ll} = 0. \tag{1.19}$$

Integrating (1.19) over the wall thickness $0 \le s \le k_0$ and recalling that a zero external pressure implies that $\mathcal{T}_{ss} = 0$ for $s = k_0$, we obtain a relation between $\mathcal{T}_{ss}(\eta)$, $\mathcal{T}_{\theta\theta}(\eta)$ and $\mathcal{T}_{ll}(\eta)$. Taking relations (1.17) into account, it is possible to obtain an explicit form for $\mathcal{T}_{ss}(\eta)$, $\mathcal{T}_{\theta\theta}(\eta)$ and $\mathcal{T}_{ll}(\eta)$. However, we will postpone this calculation after an a-dimensionalization procedure which points out the terms which are proportional to the ratio between the scales of the vessel radius and the length, which are supposed to be small and then negligible by our asymptotic analysis.

It is possible to obtain the Cauchy stress tensor T with respect to the global (cylindrical) reference frame. To this purpose it is sufficient perform a rotation around the θ-axis, that is

$$T = R\mathcal{T}R^T, \tag{1.20}$$

where the rotation matrix R is given by

$$R = \begin{bmatrix} n_r & 0 & -n_z \\ 0 & 1 & 0 \\ n_z & 0 & n_r \end{bmatrix}. \tag{1.21}$$

Here n_r and n_z are the radial and longitudinal components of the outward normal to the fluid-structure interface $\boldsymbol{n}_{\mathcal{S}}$ introduced in (1.6).

1.3 Boundary conditions at the fluid-structure interface

At the fluid-structure interface we have the continuity of the normal stresses, that is we may write

$$T_N \cdot \boldsymbol{n}_{\mathcal{S}} - T \cdot \boldsymbol{n}_{\mathcal{S}} = 0. \tag{1.22}$$

Thanks to (1.21) and the definition of the normal vector we have

$$T \cdot \boldsymbol{n}_{\mathcal{S}} = R\mathcal{T}R^T \cdot \boldsymbol{n}_{\mathcal{S}} = \begin{bmatrix} n_r \mathcal{T}_{ss} \\ 0 \\ n_z \mathcal{T}_{ss} \end{bmatrix} = c_s \begin{bmatrix} \mathcal{T}_{ss} \\ 0 \\ -\frac{\partial \eta}{\partial z}\mathcal{T}_{ss}. \end{bmatrix}$$

where we posed $\mathcal{T}_{ss} = \mathcal{T}_{ss}(\eta)$. In fact $T \cdot \boldsymbol{n}_{\mathcal{S}}$ is equal to the first column of $R\mathcal{T}$.

Relation (1.22) may then be rewritten componentwise as

$$\begin{cases} -p + \sigma_{rr} - \dfrac{\partial \eta}{\partial z}\sigma_{rz} = \varrho^{-1}\mathcal{T}_{ss}, \\ \sigma_{r\theta} - \dfrac{\partial \eta}{\partial z}\sigma_{\theta z} = 0, \\ \sigma_{rz} - \dfrac{\partial \eta}{\partial z}(-p + \sigma_{zz}) = \varrho^{-1}\left(-\dfrac{\partial \eta}{\partial z}\mathcal{T}_{ss}\right). \end{cases} \tag{1.23}$$

The term ϱ^{-1} is linked to the fact that the Navier-Stokes equations have been divided by the density. The continuity of the radial component of the velocity at the fluid-structure interface $\mathcal{S}$ implies

$$u_r = \frac{\partial \eta}{\partial t} + u_z \frac{\partial \eta}{\partial z}\,. \tag{1.24}$$

The Navier-Stokes equations (1.10) coupled with boundary conditions on $\mathcal{S}$ (1.23) and (1.24), form a consistent 3D fluid-structure interaction system (four unknowns and four boundary conditions) we will refer to throughout this paper. At this stage we will skip the problem of posing boundary conditions at the inlet and at the outlet surfaces and initial conditions. The issue will be analyzed later on for the reduced system.

1.4 Scaling the equations

We introduce the following scales: vessel length: L, vessel radius: R, u_z: V. The associated dimensionless ratios are

$$\varepsilon = \frac{R}{L}, \qquad \nu = 1/Re = \frac{\mu}{VR}, \tag{1.25}$$

where μ is the kinematic viscosity and Re is the Reynolds number, while the corresponding derived scales are u_r and u_θ: εV, p: V^2, $\mathcal{T}_{ss}, \mathcal{T}_{\theta\theta}, \mathcal{T}_{ll}$: V^2, t: L/V. The derivation of the reduced model is based on the assumption that ε be small. With an abuse of notation that however helps to reduce the number of symbols, in this section we will still denote by r, z, t, u_r, u_θ, u_z, η, p the corresponding scaled quantities. The scaled components of σ are

$$\begin{aligned} &\sigma_{rr} = 2\nu\varepsilon V^2[[D_{rr}]], \quad \sigma_{\theta\theta} = 2\nu\varepsilon V^2[[D_{\theta\theta}]], \quad \sigma_{zz} = 2\nu\varepsilon V^2[[D_{zz}]], \\ &\sigma_{r\theta} = \varepsilon\nu V^2[[D_{r\theta}]], \quad \sigma_{z\theta} = \nu V^2[[D_{z\theta}]], \quad \sigma_{rz} = \nu V^2[[D_{rz}]], \end{aligned} \tag{1.26}$$

where we posed:

$$\begin{aligned} &[[D_{rr}]] = \frac{\partial u_r}{\partial r}, \quad [[D_{\theta\theta}]] = \frac{\partial u_\theta}{\partial \theta}\frac{1}{r} + \frac{u_r}{r}, \quad [[D_{zz}]] = \frac{\partial u_z}{\partial z}, \\ &[[D_{rz}]] = \varepsilon^2\frac{\partial u_r}{\partial z} + \frac{\partial u_z}{\partial r}, \quad [[D_{r\theta}]] = r\frac{\partial}{\partial r}\left(\frac{u_\theta}{r}\right) + \frac{1}{r}\frac{\partial u_r}{\partial \theta}, \quad [[D_{z\theta}]] = \frac{1}{r}\frac{\partial u_z}{\partial \theta} + \varepsilon^2\frac{\partial u_\theta}{\partial z}. \end{aligned} \tag{1.27}$$

The only component of the elastic stress tensor that comes into play in the boundary conditions is $\mathcal{T}_{ss}/\varrho$, which scales as

$$\mathcal{T}_{ss}/\varrho = V^2[[\mathcal{T}_{ss}/\varrho]] \tag{1.28}$$

where $[[\mathcal{T}_{ss}/\varrho]]$ denotes the a-dimensional part of $\mathcal{T}_{ss}/\varrho$. Similarly we have $\mathcal{T}_{\theta\theta}/\varrho = V^2[[\mathcal{T}_{\theta\theta}/\varrho]]$ and $\mathcal{T}_{ll}/\varrho = V^2[[\mathcal{T}_{ll}/\varrho]]$.

The three-dimensional Navier-Stokes system (1.10) is now rewritten using the scaled quantities in order to put into evidence how the terms scale with ε. The continuity equation is formally unaltered, that is

$$\frac{\partial}{\partial r}(ru_r) + \frac{\partial u_\theta}{\partial \theta} + \frac{\partial}{\partial z}(ru_z) = 0. \tag{1.29}$$

After scaling and multiplication by $\dfrac{R}{V^2}$ the radial and circumferential equations become

$$\begin{aligned} &\varepsilon^2\left[\frac{\partial u_r}{\partial t} + \frac{1}{r}\frac{\partial}{\partial r}\left(ru_r^2\right) + \frac{1}{r}\frac{\partial}{\partial \theta}\left(u_r u_\theta\right) + \frac{\partial}{\partial z}(u_r u_z) - \frac{1}{r}u_\theta^2\right] = \\ &\quad -\frac{\partial p}{\partial r} + \frac{2\nu\varepsilon}{r}\frac{\partial}{\partial r}\left(r\frac{\partial u_r}{\partial r}\right) + \frac{\nu\varepsilon}{r}\frac{\partial}{\partial \theta}\left(r\frac{\partial}{\partial r}\left(\frac{u_\theta}{r}\right) + \frac{1}{r}\frac{\partial u_z}{\partial \theta}\right) + \\ &\quad + \nu\varepsilon\frac{\partial}{\partial z}\left(\frac{\partial u_r}{\partial z}\varepsilon^2 + \frac{\partial u_z}{\partial r}\right) - \frac{2\nu\varepsilon}{r^2}\left(\frac{\partial u_\theta}{\partial \theta} + u_r\right) \end{aligned} \tag{1.30}$$

and

$$\begin{aligned}\varepsilon^2\left[\frac{\partial u_\theta}{\partial t}+\frac{\partial}{\partial r}(u_r u_\theta)+\frac{1}{r}\frac{\partial}{\partial\theta}\left(u_\theta^2\right)+\frac{\partial}{\partial z}(u_\theta u_z)+\frac{2}{r}u_\theta u_r\right]= \\ -\frac{1}{r}\frac{\partial p}{\partial\theta}+\nu\varepsilon\frac{\partial}{\partial r}\left(r\frac{\partial}{\partial r}\left(\frac{u_\theta}{r}\right)+\frac{1}{r}\frac{\partial u_z}{\partial\theta}\right)+\frac{2\nu\varepsilon}{r^2}\frac{\partial}{\partial\theta}\left(\frac{\partial u_\theta}{\partial\theta}+u_r\right)+ \\ +\nu\varepsilon\frac{\partial}{\partial z}\left(\frac{1}{r}\frac{\partial u_z}{\partial\theta}+\varepsilon^2\frac{\partial u_\theta}{\partial z}\right)+\frac{2\nu\varepsilon}{r}\left(r\frac{\partial}{\partial r}\left(\frac{u_\theta}{r}\right)+\frac{1}{r}\frac{\partial u_z}{\partial\theta}\right),\end{aligned} \tag{1.31}$$

respectively. Finally, the axial momentum equation after scaling and multiplication by L/V^2 becomes

$$\begin{aligned}\frac{\partial u_z}{\partial t}+\frac{1}{r}\frac{\partial}{\partial r}(r u_r u_z)+\frac{1}{r}\frac{\partial}{\partial\theta}(u_z u_\theta)+\frac{1}{r}\frac{\partial}{\partial z}\left(r u_z^2\right)= \\ -\frac{\partial p}{\partial z}+\frac{\nu}{\varepsilon r}\frac{\partial}{\partial r}\left[r\left(\frac{\partial u_r}{\partial z}\varepsilon^2+\frac{\partial u_z}{\partial r}\right)\right]+\frac{\nu}{\varepsilon r}\frac{\partial}{\partial\theta}\left(\frac{1}{r}\frac{\partial u_z}{\partial\theta}+\varepsilon^2\frac{\partial u_\theta}{\partial z}\right)+2\nu\varepsilon\frac{\partial^2 u_z}{\partial z^2}.\end{aligned} \tag{1.32}$$

The dynamical conditions (1.23) after scaling and dividing by V^2 are equivalent to

$$\begin{cases}-p+2\nu\varepsilon[[D_{rr}]]-\varepsilon\dfrac{\partial\eta}{\partial z}\nu[[D_{rz}]]=[[\mathcal{T}_{ss}/\varrho]], \\ \varepsilon\nu[[D_{r\theta}]]-\dfrac{\partial\eta}{\partial z}\varepsilon\nu[[D_{z\theta}]]=0, \\ \nu[[D_{rz}]]-\dfrac{\partial\eta}{\partial z}\varepsilon(-p+2\nu\varepsilon[[D_{zz}]])=-\dfrac{\partial\eta}{\partial z}\varepsilon[[\mathcal{T}_{ss}/\varrho]]\end{cases} \tag{1.33}$$

And in particular the third equation in (1.33) after dividing by ε becomes:

$$\nu\left(\frac{\partial u_r}{\partial z}\varepsilon+\frac{1}{\varepsilon}\frac{\partial u_z}{\partial r}\right)+\frac{\partial\eta}{\partial z}p-2\nu\varepsilon\frac{\partial\eta}{\partial z}\frac{\partial u_z}{\partial z}=-\frac{\partial\eta}{\partial z}[[\mathcal{T}_{ss}/\varrho]] \tag{1.34}$$

The kinematic condition (1.24) remain formally unaltered.

1.5 Approximation to the first order

We now rewrite the Navier-Stokes equations (1.29)–(1.32) neglecting all the terms which are $O(\varepsilon)$. We have

$$\begin{cases}\dfrac{\partial}{\partial r}(r u_r)+\dfrac{\partial}{\partial\theta}u_\theta+\dfrac{\partial}{\partial z}(r u_z)=0 \\ \dfrac{\partial p}{\partial r}=\dfrac{\partial p}{\partial\theta}=0 \\ \dfrac{\partial u_z}{\partial t}+\dfrac{1}{r}\dfrac{\partial}{\partial r}(r u_r u_z)+\dfrac{1}{r}\dfrac{\partial}{\partial\theta}(u_z u_\theta)+\dfrac{\partial}{\partial z}(u_z^2)+ \\ \qquad+\dfrac{\partial p}{\partial z}-\dfrac{\nu}{r\varepsilon}\dfrac{\partial}{\partial r}\left(r\dfrac{\partial u_z}{\partial r}\right)-\dfrac{\nu}{r^2\varepsilon}\dfrac{\partial^2 u_z}{\partial\theta^2}=0\end{cases} \tag{1.35}$$

From (1.35) we infer that the pressure remains constant on each cross-section, as already pointed out in [2]. The axial momentum conservation equation gives information about the flow-convection; this is consistent with the fact that in long and thin vessels the flow develops mainly in the longitudinal direction.

We also rewrite here below equation (1.34), which represents the longitudinal component of the dynamical boundary conditions after scaling (1.33), with an approximation of $O(\varepsilon)$:

$$\frac{\nu}{\varepsilon}\frac{\partial u_z}{\partial r} + \frac{\partial \eta}{\partial z}p = -\frac{\partial \eta}{\partial z}[[\mathcal{T}_{ss}/\varrho]] \tag{1.36}$$

The kinematic conditions (1.24) remain identical after dropping out the terms which are $O(\varepsilon)$.

Now we evaluate with an approximation of the first order with respect to ε the component $\mathcal{T}_{ss}$ of the elastic stress tensor. We rescale (1.19), approximate to the first order, recover dimensions and integrate over the wall thickness; then we exploit relations (1.17). To this purpose, recalling (A.4) and denoting by $[[\cos\psi]]$ and by $[[\chi]]$ the rescaled expressions of $\cos\psi$ and χ, we have that:

$$[[\cos\psi]] = \left[1+\varepsilon^2\left(\frac{\partial\eta}{\partial z}\right)^2\right]^{-1/2}, \quad [[\chi]] = -\frac{\varepsilon}{L}\frac{\partial^2\eta}{\partial z^2}\left[1+\varepsilon^2\left(\frac{\partial\eta}{\partial z}\right)^2\right]^{-3/2} \tag{1.37}$$

We remark that the previous relation in addition with hypothesis of a small ϵ guarantees that h_l in (A.6) remains positive during motion. Therefore, with an approximation of the first order with respect to ε, relation (1.19) becomes:

$$\frac{\partial\left(r\mathcal{T}_{ss}\right)}{\partial s} - \mathcal{T}_{\theta\theta} = 0. \tag{1.38}$$

We now integrate for $0 \le s \le k_0$, being k_0 the thickness and recalling that $r(s) = \eta + s\cos\psi$. A zero external pressure implies that $\mathcal{T}_{ss} = 0$ outside the wall and thus we obtain that on the fluid-structure interface $\mathcal{T}_{ss}(\eta) = -\dfrac{k_0}{\eta}\mathcal{T}_{\theta\theta}(\eta)$. Since in our target applications $\eta - \eta_0$ is bounded by a quantity of the same order of magnitude as k_0 we may linearize the previous expression around $\eta = \eta_0$ and obtain

$$\mathcal{T}_{ss} = -\frac{k_0}{\eta_0}\mathcal{T}_{\theta\theta}\,. \tag{1.39}$$

From (1.17) and (1.39) we finally have that at the fluid-structure interface,

$$\mathcal{T}_{ss} = -\hat{\beta}_{ss}\frac{\eta-\eta_0}{\eta}, \quad \mathcal{T}_{\theta\theta} = \hat{\beta}_{\theta\theta}\frac{\eta-\eta_0}{\eta}, \quad \mathcal{T}_{ll} = \hat{\beta}_{ll}\frac{\eta-\eta_0}{\eta}, \tag{1.40}$$

where

$$\hat{\beta}_{\theta\theta} = \tfrac{2G}{1-C}, \quad \hat{\beta}_{ss} = \tfrac{k_0}{\eta_0}\hat{\beta}_{\theta\theta}, \quad \hat{\beta}_{ll} = C\hat{\beta}_{\theta\theta}, \tag{1.41}$$

with $C = \xi\left(1 - \dfrac{k_0}{\eta_0}\right)$. Remark that these quantities may be function of z, as the Young modulus and the reference radius η_0 may vary along the longitudinal direction. They are strictly positive under the conditions $k_0/\eta_0 < 1$ (consistent with the hypothesis of thin wall) and $\xi > 0$. We note that the relations are valid also for incompressible material $\xi = 1/2$.

We remark that the negative sign in the expression for $\mathcal{T}_{ss}$ reproduces the physical fact that an expansion of the vessel corresponds to a compression of the wall structure in the radial direction. It is worth to notice that, in accordance to [12], for thin walls we have a dominance of the circumferential stress with respect to the radial stress, since in this case $\hat{\beta}_{\theta\theta} >> \hat{\beta}_{ss}$. To ease notation, in the following we will put $\beta_{ij} = \hat{\beta}_{ij}/\varrho$.

First order approximation of the pressure. We will calculate the pressure using the dynamic condition at the interface which expresses the equilibrium of fluid and structure forces in the radial direction. By dropping out all terms which are $O(\varepsilon)$ in the first of (1.33) and recovering dimensions, we obtain that $\forall\, t \in [0,T]$ and $z \in [0,L]$,

$$p = p(\eta, z) = -\mathcal{T}_{ss}/\varrho = \beta_{ss}(z)\frac{\eta - \eta_0(z)}{\eta}. \tag{1.42}$$

Using (1.16) and (1.41) we obtain that

$$\beta_{ss}(z) = \frac{E(z)k_0}{\eta_0(z)\varrho\left[(1-\xi^2) + \xi(1+\xi)\frac{k_0}{\eta_0(z)}\right]}\,.$$

We recall that we have assumed the external pressure $p_{ext} = 0$. This is not a limitation since we can interpret p as the difference between the fluid pressure and the external pressure (what is often called *transmural* pressure). It may be convenient for the further developments to introduce the quantities $A = \pi\eta^2$ and $A_0 = \pi\eta_0^2$, which represent the measure of the vessel axial section in the current and in the reference configuration, respectively. Furthermore, for the sake of notation, we will indicate in the following β_{ss} simply by β. This way, relation (1.42) may be written in the form

$$p = \beta\left(1 - \sqrt{\frac{A_0}{A}}\right), \quad \text{where } \beta = \frac{Ek_0\sqrt{\pi}}{\varrho\sqrt{A_0}\left[(1-\xi^2) + \xi(1+\xi)\frac{k_0\sqrt{\pi}}{\sqrt{A_0}}\right]}\,. \tag{1.43}$$

With respect to the expression proposed in [14], which may be rewritten in the form

$$p = \beta_0\left(\sqrt{\frac{A}{A_0}} - 1\right), \quad \text{with } \beta_0 = \frac{Ek_0\sqrt{\pi}}{\varrho\sqrt{A_0}(1-\xi^2)}\,, \tag{1.44}$$

the differences are that (1.44) has been obtained through a linearization procedure and that the expression for β accounts also for moderately thick vessel wall, while β_0 neglects terms of the order of k_0/η_0. The latter difference is however, less relevant and may be neglected. It is easy to verify that the expression for the pressure given in (1.43) satisfies the hypothesis of admissibility illustrated in [14], namely that $p = 0$ whenever $\eta = \eta_0$ (remind that here p is the transmural pressure) and $\frac{\partial p}{\partial A} > 0$ for all $A > 0$.

Remark 1.1. *Expression (1.44) may be obtained from (1.43) by neglecting the term proportional to k_0/η_0 and taking a Young modulus function of η, namely $E = \bar{E}\frac{\sqrt{A}}{\sqrt{A_0}}$, being $\bar{E}$ a constant (possibly depending on z). This can be justified to account that large arteries tend to stiffen when expanded. This physical fact justifies to consider a general relation of the type*

$$p(A, z) = C(z)\left[\left(\frac{A}{A_0(z)}\right)^{d(z)} - 1\right], \tag{1.45}$$

where $C(z)$ and $d(z)$ are known parameters which satisfy $C(z)d(z) > 0$ and $|d| < 2$.

We obtain, as special cases, (1.43) by setting $C(z) = -\beta(z)$ and $d(z) = -\frac{1}{2}$, and (1.44) by setting $C(z) = \beta_0(z)$ and $d(z) = \frac{1}{2}$.

2 The 1D-reduced fluid-structure-interaction model

In this section we derive a one-dimensional model, performing term by term cross-section integration of the continuity equation and of the longitudinal momentum equation in (1.35). The pressure is assigned through formula (1.42). We will use the following notation.

Notation 2.1. *Let $f : [0, T] \times \mathbb{R}^+ \times [0, 2\pi) \times [0, L] \to \mathbb{R}$. Then:*

$$\bar{f}(t, z) \doteq \int_0^{2\pi}\int_0^{\eta} f(t, r, \theta, z) r dr d\theta, \quad \overline{\overline{f}}(t, z) \doteq \frac{1}{\pi\eta^2}\bar{f}(t, z)\,.$$

Remark 2.1. Observe that, if $g : [0, T] \times \mathbb{R}^+ \times [0, 2\pi) \times [0, L] \to \mathbb{R}$ is a sufficiently smooth function, the following identities hold:

$$\overline{\frac{\partial g}{\partial t}} = \frac{\partial \overline{g}}{\partial t} - \eta\frac{\partial \eta}{\partial t}\int_0^{2\pi} g_{|r=\eta} d\theta, \quad \overline{\left(\frac{1}{r}\frac{\partial (rg)}{\partial r}\right)} = \eta\int_0^{2\pi} g_{|r=\eta}\, d\theta\,.$$

Moreover, if g is continuous w.r.t. the coordinate θ, for any $\alpha \in \mathbb{R}$

$$\overline{\left(r^\alpha\frac{\partial g}{\partial \theta}\right)} = \int_0^{\eta} r^{\alpha+1}\left(\int_0^{2\pi}\frac{\partial g}{\partial \theta}\, d\theta\right) dr = 0, \quad \overline{\left(r^\alpha\frac{\partial g}{\partial z}\right)} = \frac{\partial}{\partial z}\overline{g r^\alpha} - \eta^{\alpha+1}\frac{\partial \eta}{\partial z}\int_0^{2\pi} g_{|r=\eta}\, d\theta\,.$$

Averaging the continuity equation. Let us consider the continuity equation in (1.35) and average each term on the cross-section. Then, using the expressions in Remark 2.1 and taking (1.24) we obtain that

$$\frac{\partial(\eta^2)}{\partial t} + \frac{\partial(\eta^2\overline{\overline{u_z}})}{\partial z} = 0. \tag{2.1}$$

Assumptions on the velocity profile We will assume that

$$\overline{\overline{u_z}}^2(t,z) - \overline{\overline{u_z^2}}(t,z) = O(\varepsilon).$$

This implies that the velocity profile is mainly flat.

Averaging the axial momentum equation. Let us first consider the convective term of the axial momentum equation in (1.35) and average each term on the cross-section. Then, thanks to Remark 2.1, taking (1.24) into account, in view of the assumption on the velocity and dropping out the terms which are $O(\varepsilon)$, we may write

$$\frac{\partial(\eta^2\overline{\overline{u_z}})}{\partial t} + \frac{\partial\left(\eta^2\overline{\overline{u_z^2}}\right)}{\partial z} = \frac{\partial(\eta^2\overline{\overline{u_z}})}{\partial t} + \frac{\partial\left(\eta^2\overline{\overline{u_z}}^2\right)}{\partial z}. \tag{2.2}$$

The remaining terms after averaging give

$$\frac{\partial}{\partial z}\int_0^{2\pi}\int_0^{\eta} pr dr d\theta - \int_0^{2\pi} \eta\left[\frac{\partial\eta}{\partial z}p + \nu\frac{\partial u_z}{\partial r}\frac{1}{\varepsilon}\right]_{|r=\eta} \quad d\theta \tag{2.3}$$

Taking the first-order approximation of the continuity of the axial stress at the fluid-structure interface (1.36) into account, we may replace the last term of (2.3) as:

$$\int_0^{2\pi} \eta\left[\frac{\partial\eta}{\partial z}p + \nu\frac{\partial u_z}{\partial r}\frac{1}{\varepsilon}\right]_{|r=\eta} d\theta = \int_0^{2\pi} \eta(-\frac{\partial\eta}{\partial z}[[\mathcal{T}_{ss}]]/\varrho) \quad d\theta, \tag{2.4}$$

where the pressure is given by (1.42) and the radial component of the local elastic stress tensor have been assigned in (1.40).

Remark 2.2. *Sometimes one accounts for a different velocity profile by introducing a coefficient in the quadratic advective term, the so-called momentum correction coefficient, like in [14]. However, this is not the route we have followed here. Indeed, the correct value of the coefficient is difficult to be found in general. Moreover, it has been found that in haemodinamic applications its value would be in practice proximal to one [16], and its influence in the solution is negligible.*

For the sake of notation we will indicate in the following $u = \overline{\overline{u_z}}$.

The 1D model. Using (2.1)–(2.4) and recovering dimensions, in terms of the variables

$$A \doteq \pi\eta^2, \qquad Q \doteq \pi\eta^2 u = Au\,,$$

after simple computations we obtain the following reduced model on $(0,T)\times(0,L)$:

$$\begin{cases} \dfrac{\partial A}{\partial t} + \dfrac{\partial Q}{\partial z} = 0 \\ \dfrac{\partial Q}{\partial t} + \dfrac{\partial}{\partial z}\left(\dfrac{Q^2}{A}\right) + A\dfrac{\partial p}{\partial z} = 0 \\ p(A,z) = C(z)\left[\left(\dfrac{A}{A_0(z)}\right)^{d(z)} - 1\right] \end{cases} \tag{2.5}$$

with $d = -1/2$ and $C(z) = -\beta(z)$, see (1.43) and Remark 1.1.

Remark 2.3. *In the one dimensional model proposed in [14] and in many other similar models a zeroth-order term is present due to the treatment of the viscous term in the boundary layer. Its derivation required to assume a velocity profile. Here this term is not present because of the way the balance at the fluid-structure interface has been set up. The price to pay is the lack of an explicit imposition of a no-slip condition at the interface. If necessary, the zeroth-order term may be added a-posteriori following heuristic arguments. However, we wish to point out that the hyperbolic one dimensional model model is valid only when the propagative effects are dominant with respect to the viscous ones. Therefore the addition of the zeroth order term should not change substantially the behavior of the solution.*

3 Mathematical analysis

In this section we write a conservation form and point out some analytical properties of the system (2.5). Then, in the constant coefficients case, we prove a general theorem which guarantees the global in time existence of regular solutions on a finite space for a reducible quasilinear system of two hyperbolic equations with suitable boundary conditions and show how models (2.5) may fit this theory.

The conservation form. In terms of variables A and Q on the time-space domain $[0,T]\times[0,L]$, the conservation form of the system (2.5) is given by:

$$\begin{cases} \dfrac{\partial A}{\partial t} \;+\; \dfrac{\partial Q}{\partial z} = 0 \\ \dfrac{\partial Q}{\partial t} \;+\; \dfrac{\partial}{\partial z}\left(\dfrac{Q^2}{A} + \dfrac{Cd}{A_0^d(d+1)}A^{d+1}\right) = S(z,A) \end{cases} \tag{3.1}$$

where $Cd > 0$, $|d| < 2$, $d \neq -1$, $A > 0$, $A_0 > 0$. The source term depends on the known parameters $C(z)$, $d(z)$, $A_0(z)$ and vanishes if these parameters are constant. Its explicit form may be derived following the computations exposed in [14]. If we use expression (1.43) for the pressure term, the source term becomes

$$S(z,A) = \beta\sqrt{\frac{A}{A_0}}\frac{dA_0}{dz} + \sqrt{A}\left(2\sqrt{A_0} - \sqrt{A}\right)\frac{d\beta}{dz}\,.$$

The eigenvalues. The Jacobian of the flux in the system (3.1) is given by:

$$\begin{bmatrix} 0 & 1 \\ -\dfrac{Q^2}{A^2} + c_1^2 & \dfrac{2Q}{A} \end{bmatrix}, \tag{3.2}$$

$$c_1(z,A) = \sqrt{Cd}\left(\tfrac{A}{A_0}\right)^{\frac{d}{2}} \tag{3.3}$$

and the eigenvalues are given by:

$$\gamma(z,A,u) = u - c_1, \qquad \mu(z,A,u) = u + c_1\,. \tag{3.4}$$

We refer to the quantity c_1, (3.3), as the *characteristic speed*. Since we required $Cd > 0$, the eigenvalues are well defined for $A, A_0 > 0$ and real with $\mu > \gamma$ and then the system (3.1) is strictly hyperbolic. Moreover, the system is genuinely nonlinear; indeed,

$$R_\gamma = -[1,\gamma]^t, \qquad R_\mu = [1,\mu]^t$$

are right eigenvectors of (3.2); now, setting $U = [A,Q]^t$, we compute that

$$\nabla_U\gamma\cdot R_\gamma \;=\; \nabla_U\mu\cdot R_\mu \;=\; \frac{\partial c_1}{\partial A} \;+\; \frac{c_1}{A} = \frac{c_1}{A}\left(1+\frac{d}{2}\right) > 0 \quad \text{since } |d|<2\,.$$

The Riemann invariants. Following [4], chap. VII, we compute the two Riemann invariants associated to the system (3.1), as the scalar functions $r(z,U)$, $s(z,U)$ such that:

$$\frac{\partial r}{\partial U} = L_\gamma, \quad \frac{\partial s}{\partial U} = L_\mu$$

where L_γ, L_μ are the left eigenvectors of the matrix (3.2):

$$L_\gamma(z,A,u) = [-\mu, 1]\xi(A,Q), \qquad L_\mu(z,A,u) = [-\gamma, 1]\xi(A,Q)$$

and $\xi(A,Q)$ is a scalar smooth function of its arguments. Choosing $\xi(A,Q) = 1/A$ we find

$$r(z,U) \;=\; u - F, \qquad s(z,U) \;=\; u + F, \qquad F = F(z,A) \;=\; \textstyle\int_{A_0}^{A} \frac{c_1(z,\alpha)}{\alpha}\, d\alpha\,. \tag{3.5}$$

Since $\partial F/\partial A = c_1/A = (2/d)(\partial c_1/\partial A)$, (observe that $\partial F/\partial A > 0$), we find that

$$F(z,A) = \frac{2\sqrt{Cd}}{d}\left[\left(\frac{A}{A_0}\right)^{\frac{d}{2}} - 1\right] \tag{3.6}$$

Using (3.5) and (3.6), we can express u and c_1 in terms of r, s as follows:

$$u = \frac{r+s}{2}\,, \qquad c_1 = \frac{d}{4}(s-r) + \sqrt{Cd}\,.$$

Thanks to the previous relations, we have that:

$$\gamma = \frac{r(2+d) + s(2-d)}{4} - \sqrt{Cd}, \qquad \mu = \frac{r(2-d) + s(2+d)}{4} + \sqrt{Cd} \tag{3.7}$$

We remark that in order to have satisfied the subcritical condition $\gamma < 0 < \mu$, it is sufficient that $|r|, |s| < \sqrt{Cd}$.

In Riemann coordinates, the system(3.1) rewrites as

$$\begin{cases} \dfrac{\partial r}{\partial t} + \gamma(z,r,s)\dfrac{\partial r}{\partial z} = E_1(z,r,s) \\[2ex] \dfrac{\partial s}{\partial t} + \mu(z,r,s)\dfrac{\partial s}{\partial z} = E_2(z,r,s) \end{cases} \tag{3.8}$$

with suitable E_1 and E_2.

3.1 The special case where the parameters are constant

From now on, we assume that the parameters A_0, C and d are constant. The source terms in (3.1) vanish and the system becomes homogeneous; the diagonal system (3.8) rewrites as

$$\begin{cases} \dfrac{\partial r}{\partial t} + \gamma(r,s)\dfrac{\partial r}{\partial z} = 0 \\[2ex] \dfrac{\partial s}{\partial t} + \mu(r,s)\dfrac{\partial s}{\partial z} = 0\,. \end{cases} \tag{3.9}$$

We provide the system (3.9) with initial data

$$(r,s)(0,z) = (r_0(z), s_0(z)) \,, \qquad z \in [0,L] \tag{3.10}$$

and boundary conditions

$$z = 0: \qquad s(t,0) = k \cdot r(t,0) + v(t)\,, \qquad k = \pm 1\,, \tag{3.11}$$

$$z = L: \qquad r(t,L) = 0\,. \tag{3.12}$$

We analyze the mixed IBV problem (3.9)–(3.12), with k either -1 or 1, for smooth data. We can apply a result by Li, Rao and Jin, ([18], Theorem 2.1) concerning semiglobal solutions – that is, for any prescribed $\tau > 0$, a smooth unique solution exists up to time τ, provided that the C^1 norm of the initial data is sufficiently small. The result in [18] is valid for boundary conditions which include (3.11), (3.12). Here, due to our special boundary conditions (especially (3.12)), we can prove that the solution to our problem is defined globally in time.

Theorem 3.1. *Assume that γ, μ are C^1 functions of r, s and that $\mu(r,s) > 0 > \gamma(r,s)$ for all (r,s). Assume that r_0, $s_0 \in C^1([0,L])$, $v \in C^1([0,+\infty))$, $\|v\|_{C^0([0,\infty))} < +\infty$ and that the compatibility conditions are satisfied:*

$$z = 0: \qquad \begin{cases} s_0(0) = k r_0(0) + v(0) \quad \textit{where} \quad k = \pm 1, \\ \mu(r_0(0), s_0(0)) s_0'(0) = k\gamma(r_0(0), s_0(0)) r_0'(0) - v'(0) \end{cases} \tag{3.13}$$

$$z = L: \qquad r_0(L) = 0, \quad r_0'(L) = 0 \tag{3.14}$$

Then, the mixed IBV problem (3.9)–(3.12), with either $k = -1$ or $k = 1$, together with (3.13), (3.14), admits a unique C^1 solution on $[0,+\infty) \times [0,L]$, provided that

$$b_0 \doteq \max\left\{ \left\| \left(\frac{\partial r_0}{\partial z}, \frac{\partial s_0}{\partial z} \right) \right\|_{C^0([0,L])}, \left\| \frac{\partial v}{\partial t} \right\|_{C^0([0,+\infty))} \right\}$$

is small enough. In particular, if we pose

$$a_0 \doteq \max\left\{ \|s_0\|_{C^0([0,L])}, \|r_0\|_{C^0([0,L])} + \|v\|_{C^0([0,\infty))} \right\}, \tag{3.15}$$

we have:

$$|r(t,z)|, \ |s(t,z)| \ \leq \ a_0, \qquad \forall\, t,\, z \tag{3.16}$$

$$\left\| \left(\frac{\partial r}{\partial z}(t,\cdot), \frac{\partial s}{\partial z}(t,\cdot) \right) \right\|_{C^0([0,L])} \ \leq \ C(b_0), \qquad \forall\, t > 0 \tag{3.17}$$

where $C(b_0)$ is a positive constant which vanishes as $b_0 \to 0$.

Moreover, if the boundary data $v : [0, +\infty) \to \mathbb{R}$ is periodic, the solution becomes periodic in time: there exists $T > 0$ such that $(r(t, z), s(t, z))$ is periodic in time on the set $[T, \infty) \times [0, L]$.

Proof. Recalling the definition of a_0, (3.15), choose $M > a_0$ and define

$$M_0 \quad = \quad \max_{|r|,|s|\leq M} \left\{ \frac{1}{|\gamma(r,s)|}, \ \frac{1}{\mu(r,s)} \right\} . \tag{3.18}$$

Then choose a time $T > 0$. By Theorem 2.1 in [18], the initial-boundary value problem (3.9)–(3.14) admits a unique C^1 solution $(r(z,t), s(z,t))$ in the domain $D_T = \{(t, z) : \ 0 \leq t \leq T\,, \quad 0 \leq z \leq L\}$, provided that the C^1 norms of r_0, s_0, v are small enough. Moreover, there exists a positive constant $C_2(T, b_0)$ such that $\left\| \left(\frac{\partial r}{\partial z}(t, \cdot), \frac{\partial s}{\partial z}(t, \cdot) \right) \right\|_{C^0([0,L])} \leq C_2(T, b_0)$.

Recall that r is constant along γ-characteristics and s is constant along μ-characteristics. Let us refine the estimates on r, s.

Estimates on r. Let $(t_o, z_o) \in D_T$. Consider the γ-characteristic passing through (t_o, z_o), for $t < t_o$. Then, one of the two following situations occurs. Either it intersects the z-axis at some point $(0, \alpha)$, and then

$$|r(t_o, z_o)| = |r(0, \alpha)| \leq \|r_0\|_{C^0([0,L])}\,,$$

or it intersects the right boundary $z = L$ at some time $\tau < t_o$, and then

$$|r(t_o, z_o)| = |r(\tau, L)| = 0\,.$$

Then one has

$$|r(t, z)| \leq \|r_0\|_{C^0([0,L])}, \qquad \forall\, (t, z) \in D_T\,. \tag{3.19}$$

Estimates on s. Let us now consider the μ-characteristic passing through (t_o, z_o). If it reaches the z-axis at $t = 0$, at some point $(0, \alpha)$, then

$$|s(t_o, z_o)| = |s(0, \alpha)| \leq \|s_0\|_{C^0([0,L])}\,,$$

while if it intersects the left boundary at some point $(\tau, 0)$, one has

$$|s(t_o, z_o)| = |s(\tau, 0)| = |kr(\tau, 0) + v(\tau)| \leq \|r_0\|_{C^0([0,L])} + \|v\|_{C^0([0,\infty))}\,,$$

where we have used the bound on r, (3.19). We can conclude that

$$|s(t,z)| \leq \max\{\|s_0\|_{C^0([0,L])}, \|r_0\|_{C^0([0,L])} + \|v\|_{C^0([0,\infty))}\} = a_0 \qquad \forall\, (t,z) \in D_T\,. \tag{3.20}$$

Putting together (3.19), (3.20), we find

$$|r(t,z)|,\ |s(t,z)| \leq a_0 < M, \qquad \forall\, (t,z) \in D_T\,. \tag{3.21}$$

Observe that this last estimate does not depend on T; hence, to obtain the C^0 estimate on r, s, we do not need to require a_0 to be small. Moreover, following the proof in [18], the estimate on the derivatives does not depend on the smallness of a_0 (the constant A_1 that appears there is equal to 0 in our case) but only on the smallness of b_0.

Next, choose T as follows:

$$T \ = \ 2LM_0\,. \tag{3.22}$$

Let $z_1(t)$ be the γ-characteristic starting at the point $(t=0, z=L)$. It exists up to some time $T_1 > 0$, time at which it intersect the left boundary $z = 0$. Observe that

$$T_1 \ \leq \ L \cdot \max_{|r|,|s|\leq M} \frac{1}{|\gamma(r,s)|} \leq LM_0 = \frac{T}{2}\,, \tag{3.23}$$

thanks to our choice of T. Then one has, if $(t,z) \in D_T$:

$$\begin{aligned} |r(t,z)| &\leq a_0 \qquad && \text{if } z \leq z_1(t), \quad t \in [0,T_1] \\ r(t,z) &\equiv 0 \qquad && \text{if } z > z_1(t), \quad t \in [0,T_1] \quad \text{or if} \quad t \in (T_1,T], \quad z \in [0,L]\,. \end{aligned}$$

In particular, $r(T,z) \equiv 0$ for all $z \in [0,L]$. Now, let $z_2(t)$ be the μ-characteristic issued at $(T_1, 0)$; it will intersect the right boundary at some time $T_2 > T_1$. Observe that T_2 satisfies

$$T_2 - T_1 \ \leq \ L \cdot \max_{|r|,|s|\leq M} \frac{1}{\mu(r,s)}\,, \tag{3.24}$$

that gives, together with (3.23), $T_2 \ \leq \ 2LM_0 \ = \ T$.

By the previous analysis on s, we deduce the following. If (t_o, z_o) lies above the graph of $z_2(t)$, then the μ-characteristic issued at (t_o, z_o) intersect the left boundary at some time $\tau \geq T_1$, and then, since $r(\tau, 0) = 0$, the left boundary condition reduces to

$$s(\tau, 0) = v(\tau) \qquad \forall\, \tau \geq T_1\,.$$

In conclusion we have, for $(z,t) \in D_T$,

$$|s(t,z)| \leq \begin{cases} a_0 & \text{if } z \geq z_2(t), \quad t \in [T_1, T_2] \\ \\ \|v\|_{C^0([0,\infty))} & \text{if } z < z_2(t), \quad t \in [T_1, T_2] \quad \text{or} \quad t \in (T_2, T], \quad \forall\, z \in [0, L]\,. \end{cases}$$

After time T, the solution can be continued as follows: $r \equiv 0$, while s is completely determined by the left boundary data v. If the C^1 norm of v is small enough, a C^1 solution s of

$$s_t + \mu(0,s)s_z = 0, \qquad s(t,0) = v(t)$$

exists for all (t,z), $t \geq T$, $z \in [0,L]$. Therefore, the inequality on the derivatives of the solution holds globally on time. □

The IBV problem. Next, we are going to apply Theorem 3.1 to the system (3.1), which written in the physical variables reads as

$$\begin{cases} \dfrac{\partial A}{\partial t} \; + \; \dfrac{\partial Q}{\partial z} = 0 \\ \dfrac{\partial Q}{\partial t} \; + \; \dfrac{\partial}{\partial z}\left(\dfrac{Q^2}{A} + \dfrac{Cd}{A_0^d(d+1)} A^{d+1}\right) \; = \; 0 \end{cases} \tag{3.25}$$

where here C, $d \neq -1$ and A_0 are constant. To this purpose, we need to prove that, for all (t,z), A remains positive and that $\gamma(A,u) < 0 < \mu(A,u)$.

Remark 3.1. *We point out that system (3.25) in the case $d \geq 0$ reduces to the classical p-system of gas-dynamics with $\gamma = d+1$.*

The property that A does not vanish is essential: if $d > 0$ as in the model proposed in [14] it guarantees strict hyperbolicity, while if $d < 0$, as in the model here derived, it is needed to have the eigenvalues (3.4) well defined.

We provide the system (3.1) with initial conditions

$$A(0,z) = A_0, \qquad u(0,z) = u_0(z), \qquad z \in [0,L]\,. \tag{3.26}$$

As for the boundary conditions, we prescribe at $z = 0$ either the vessel area $A(0,t) = A_{in}(t)$ or the velocity $u(0,t) = u_{in}(t)$, while at the outlet boundary $z = L$ we impose a non-reflecting boundary condition, that is we require that the backward characteristic vanishes. Thus, we consider either

$$z = 0: \quad A(t,0) = A_{in}(t)\,; \qquad z = L: \quad u(t,L) - F(A(t,L)) = 0, \quad t > 0 \tag{3.27}$$

or

$$z = 0 : \quad u(t,0) = u_{in}(t)\,; \qquad z = L : \quad u(t,L) - F(A(t,L)) = 0, \quad t > 0 \tag{3.28}$$

where $F(A) = \frac{2\sqrt{Cd}}{d}\left[\left(\frac{A}{A_0}\right)^{\frac{d}{2}} - 1\right]$.

Proposition 3.1. **(I)** *We consider the IBV problem (3.25)–(3.27) with $A_{in} : [0,+\infty) \to \mathbb{R}^+$ of class C^1. Let $A_0 > 0$, $u_0 \in C^1([0,L])$ and assume the following compatibility conditions:*

$$u_0(L) = u_0'(L) = 0, \qquad A_{in}(0) = A_0, \qquad A_0 u_0'(0) + A_{in}'(0) = 0\,. \tag{3.29}$$

Moreover assume that

$$\|u_0\|_{C^0([0,L])} + 2\,\|F(A_{in})\|_{C^0([0,\infty))} \;<\; \sqrt{Cd} \tag{3.30}$$

and that $\left\|\frac{\partial A_{in}}{\partial t}\right\|_{C^0([0,+\infty))}$, $\left\|\frac{\partial u_0}{\partial z}\right\|_{C^0([0,L])}$ are sufficiently small.

Then, the IBV problem (3.25)–(3.27) admits a unique C^1 solution $(A(t,z), u(t,z))$ on $[0,\infty) \times [0,L]$. Moreover, if the left boundary data is periodic, the solution eventually becomes periodic in time.

(II) *We consider the IBV problem (3.25), (3.26), (3.28) with $u_{in} : [0,+\infty) \to \mathbb{R}$ of class C^1. Let $A_0 > 0$, $u_0 \in C^1([0,L])$ and assume the compatibility conditions:*

$$u_0(L) = u_0'(L) = 0, \qquad u_{in}(0) = u_0(0), \qquad u_0(0)u_0'(0) + u_{in}'(0) = 0\,. \tag{3.31}$$

Moreover assume that

$$\|u_0\|_{C^0([0,L])} + 2\,\|u_{in}\|_{C^0([0,\infty))} \;<\; \sqrt{Cd} \tag{3.32}$$

and that $\left\|\frac{\partial u_{in}}{\partial t}\right\|_{C^0([0,+\infty))}$, $\left\|\frac{\partial u_0}{\partial z}\right\|_{C^0([0,L])}$ are sufficiently small.

Then, the same conclusion of **(I)** *holds for the IBV problem (3.25), (3.26), (3.28).*

Proof. We pass to the Riemann coordinates, (3.5), and check the assumptions of Theorem 3.1. Since $F(A_0) = 0$, we have

$$r_0(z) = s_0(z) = u_0(z)\,. \tag{3.33}$$

For both (3.27), (3.28) the boundary condition at $z = L$ rewrites as $r = 0$, see (3.12). At $z = 0$, condition (3.27) (case **(I)**) becomes

$$s(t,0) = r(t,0) + v(t), \qquad v(t) = 2F\left(A_{in}(t)\right)$$

while condition (3.28) (case **(II)**) becomes

$$s(t,0) = -r(t,0) + v(t), \qquad v(t) = 2u_{in}(t)\,.$$

Hence we are dealing with the IBV problem (3.9)–(3.11) for the diagonal system, with $k = \pm 1$. Recalling (3.7), the condition $\gamma < 0 < \mu$ is equivalent to require that

$$\frac{r(2+d) + s(2-d)}{4} \;<\; \sqrt{Cd}\,, \qquad\qquad \frac{r(2-d) + s(2+d)}{4} \;>\; -\sqrt{Cd}\,. \tag{3.34}$$

At time $t = 0$, (3.34) is satisfied, thanks to (3.33), (3.30), (3.32). Moreover, one can easily verify that (3.29), (3.31) give the compatibility conditions (3.13), (3.14) for both cases $k = \pm 1$.

Hence, by Theorem 3.1, a C^1 solution of the diagonal system (3.9), satisfying our initial, boundary and compatibility conditions, exists and, correspondingly, also a C^1 solution (A, u) for the system (3.25), as soon as $\gamma < 0 < \mu$ and $A > 0$. We must show that these conditions are verified for all $t > 0$.

Observe that the quantity a_0, introduced at (3.15), here amounts either to

$$a_0 = \|u_0\|_{C^0([0,L])} + 2\,\|F(A_{in})\|_{C^0([0,\infty))} \quad \text{(case } \mathbf{(I)}\text{)} \tag{3.35}$$

or to

$$a_0 = \|u_0\|_{C^0([0,L])} + 2\,\|u_{in}\|_{C^0([0,\infty))} \quad \text{(case } \mathbf{(II)}\text{)}$$

which is in both cases $< \sqrt{Cd}$ by assumptions (3.30), (3.32), respectively.

Recalling (3.16), until the (r, s)–solution exists, it must be

$$\frac{r(2+d) + s(2-d)}{4} \le a_0 < \sqrt{Cd}\,, \qquad \frac{r(2-d) + s(2+d)}{4} \ge -a_0 > -\sqrt{Cd}\,. \tag{3.36}$$

Hence (3.34) is satisfied. Moreover, recalling that

$$u = \frac{r+s}{2}\,, \qquad F(A) = \frac{s-r}{2}$$

we obtain $|u(t,z)| \le\; a_0 \;<\; \sqrt{Cd}$.

To show that A is well defined, we need to invert F. Recall that F is strictly increasing; moreover if $d < 0$ $F(A) \to -\infty$ as $A \to 0+$ and $F(A) \to 2\sqrt{C/d}$ as $A \to +\infty$, while if $d > 0$ $F(A) \to +\infty$ as $A \to +\infty$, and $F(A) \to -2\sqrt{C/d}$ as $A \to 0+$. Recalling that $|d| < 2$ and $Cd > 0$, we have

$$|F(A)| = \left|\frac{s-r}{2}\right| \;\le\; \frac{|s| + |r|}{2} \;\le\; a_0 < \;\sqrt{Cd} \;<\; 2\sqrt{\frac{C}{d}}\,; \tag{3.37}$$

we deduce that A is well defined and is bounded away from 0. Hence the solution in the (r,s)–variables, and, correspondingly, in the (A,u)–variables, is well defined for all $t>0$. □

Remark 3.2. We can give estimates for $A(t,z)$ $u(t,z)$ in terms of the parameters and the data. First of all, the assumption (3.32) implies necessarily that $|u_o(z)| \le \sqrt{Cd}$, $|u_{in}(t)| \le \sqrt{Cd}/2$ while, recalling the definition of $F(A)$, the assumption (3.30) implies that

$$\left(\frac{4-d}{4}\right)^{\frac{2}{d}} < \frac{A_{in}(t)}{A_0} < \left(\frac{4+d}{4}\right)^{\frac{2}{d}}.$$

From (3.37), we deduce that $|u(t,z)|$, $|F(A(t,z)| \le \sqrt{Cd}$ and then

$$\left(\frac{2-d}{2}\right)^{\frac{2}{d}} < \frac{A(t,z)}{A_0} < \left(\frac{2+d}{2}\right)^{\frac{2}{d}}.$$

Recalling the proof of Theorem 3.1, after a time $T>0$ one has $r\equiv 0$, hence $u=F(A)=s/2$. Then, the estimates

$$\left(\frac{4-d}{4}\right)^{\frac{2}{d}} < \frac{A(t,z)}{A_0} < \left(\frac{4+d}{4}\right)^{\frac{2}{d}}, \qquad |u(t,z)| \le \frac{\sqrt{Cd}}{2} \qquad \forall\, t \ge T \tag{3.38}$$

can be easily obtained.

We can give a lower bound on the time T after which the solution depends only on the left boundary data.

In fact from (3.22), (3.18), (3.7) and (3.16) we have that:

$$T \ge \frac{2L}{\sqrt{Cd}-a_0}. \tag{3.39}$$

We remark that, as the length L increases, the time T will increase and, consequently, we will need a smaller bound on the derivatives of the data, when applying Theorem 3.1.

In the case of the model derived here, where the pressure is given by (1.43), we have $d=-\frac{1}{2}$ and then $F(A)=2\sqrt{2\beta}\left(1-\sqrt[4]{A_0/A}\right)$. Therefore $0.41 \approx (4/5)^4 < A(t,z)/A_0 < (4/3)^4 \approx 3.16$, and $|u|<\sqrt{\beta/2}$ while after a time T which satisfies inequality (3.39) one has:

$$0.62 \approx \left(\frac{8}{9}\right)^4 < \frac{A(t,z)}{A_0} < \left(\frac{8}{7}\right)^4 \approx 1.7, \qquad |u| < \sqrt{\frac{\beta}{8}}$$

In the case of the model with pressure given by (1.44), we have that $d=\frac{1}{2}$ and then $F(A)=2\sqrt{2\beta_0}\left(\sqrt[4]{\frac{A}{A_0}}-1\right)$. Therefore $0.31 \approx (3/4)^4 < \frac{A(t,z)}{A_0} < (5/4)^4 \approx 2.44$ and $|u|<\sqrt{\beta_0/2}$, while after a suitable time T one has:

$$0.59 \approx \left(\frac{7}{8}\right)^4 < \frac{A(t,z)}{A_0} < \left(\frac{9}{8}\right)^4 \approx 1.6, \qquad |u| < \sqrt{\frac{\beta_0}{8}}.$$

4 Numerical results

In this section we present a numerical validation of model governed by the pressure relation (1.43) (here referred for simplicity as the "new model"), comparing it with the numerical results obtained by the model introduced in [14], in the inviscid case. We consider the case where all the parameters are constant, this allows us to verify numerically the bounds of the theorem. For both models, we set $A(0,z) = A_0 > 0$, $Q(0,z) = 0$, $z \in [0,L]$. At the left boundary $z = 0$ we impose an area variation given by

$$A_{in}(t) = A_0(1 + 0.1\sin(2\pi t/T_{per})), \quad t > 0$$

which guarantees that $\frac{A_{in}(t)}{A_0} \in [0.9, 1.1]$, $\forall\, t \geq 0$ and that $\left\| \frac{\partial A_{in}}{\partial t} \right\|_{C^0([0,+\infty))} \leq \frac{0.2\cdot\pi\cdot A_0}{T_{per}}$. At the right boundary $z = L$ we are imposing that the incoming characteristic variable is zero. We are then in the condition of Theorem 3.1 (assuming that the time derivatives are small enough).

To discretize the two models we have adopted the second order Taylor-Galerkin scheme described in [10], which is an accurate numerical scheme in the case of smooth solutions. The scheme has been implemented using the lifeV finite element library (www.lifev.org).

We consider a uniform mesh on the space and time intervals.

The data in the unit system CGS (centimeters, grams, seconds) are

$$\begin{aligned} &L = 60, \quad \Delta z = 1, \quad \Delta t = 0.0001, \\ &E = 4 \cdot 10^6, \quad k_0 = 0.065, \quad \xi = 0.5 \\ &A_0(z) = 1.76715, \quad u_0(z) = 0 \quad z \in [0,L], \quad T_{per} = 0.8, \\ &\varrho = 1. \end{aligned} \tag{4.1}$$

It can be verified that our initial and boundary data satisfy the assumptions of Proposition 3.1, for both models. Then the subcritical condition (i.e. $|u| < c_1$)) is everywhere satisfied during the motion. The numerical solution shows a smooth curve for both the cross-section area and the velocity (see Figures 4 and 5), confirming that in this test case the data have been taken small enough.

If we compare the characteristic speed for the new model and for the old model when $A = A_0$, we have

$$\textbf{char-speed-new} = \sqrt{\frac{\beta}{2}} \approx 461.17, \qquad \textbf{char-speed-old} = \sqrt{\frac{\beta_0}{2}} \approx 480.74, \tag{4.2}$$

which show that the two models are almost equivalent, with a slight slower propagation speed for the new one.

As our numerical test fits the hypotheses of Proposition 3.1 - case **(I)**, using (4.1) we may compute through (3.39) the minimum time T, referred to as "critical time" after which the solution depends only on the left boundary condition, for the new and for the old model, respectively:

$$T_{new} = 0.3206, \qquad T_{old} = 0.3093. \tag{4.3}$$

We compare at $t = 0.1, 0.3, 0.5, 0.7$ the cross-section area in Figure 4 and the velocity in Figure 5 for both the new and the old model and remark that the numerical results are quite similar for the areas, while there are slight differences for the velocity; in fact the two models have a different expression for the current characteristic speed (3.3). In the new model the coefficient $d = -\frac{1}{2} < 0$, causes a decrement of the characteristic speed with the increase of A, which is consistent with the elastic behavior. The old model has an opposite behavior, being $d = \frac{1}{2} > 0$. This could be more appropriate to simulate the stiffening characteristics of the wall of large arteries. In the following table we display the values of the C^0-norm of the ratio A/A_0 and of the velocity at the given times, in order to verify if the bounds prescribed in Remark 3.2 are satisfied for both models, before and after the times (4.3), respectively:

t	$\left\|\frac{A_{\text{new}}(t,\cdot)}{A_0}\right\|_{C^0([0,L])}$	$\|u_{\text{new}}(t,\cdot)\|_{C^0([0,L])}$	$\left\|\frac{A_{\text{old}}(t,\cdot)}{A_0}\right\|_{C^0([0,L])}$	$\|u_{\text{old}}(t,\cdot)\|_{C^0([0,L])}$
0.1	1.0344	15.51	1.0345	14.19
0.3	1.0477	21.68	1.0479	19.98
0.5	1.0112	17.01	1.0157	15.01
0.7	0.9635	24.67	0.9637	21.82

If we recall the values of the characteristic speed for both models (4.2), we may conclude that the bounds prescribed in Remark 3.2 are satisfied at the given times.

5 Conclusions and further developments

In this paper we have obtained a one-dimensional system describing the mean axial motion of a Newtonian incompressible fluid moving into a compliant straight vessel and the radial displacement of its isotropic and linearly elastic wall. The methodology can be extended to account for curvature and torsion. This extension is the subject of current research.

The analysis has demonstrated the well posedness of the problem under realistic data. This has been confirmed by numerical experiments. Work is ongoing to extend the results to other type of boundary conditions relevant to the practice and to derive quantitative bounds on the derivatives of the inlet data which guarantee smooth solution of models (2.5).

A The metric of the wall

In Figure 3 an axial section of the vessel at a given time $t \in [0, T]$ is presented.

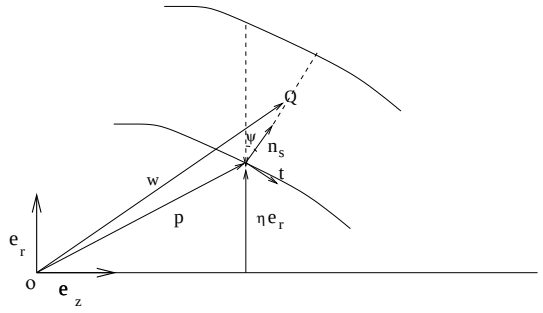

Figure 3: An axial section of the vessel at a given time t

Let us consider the vector-position of a point at the fluid-structure interface at a fixed time t given by:

$$p(t, \theta, z) = z\boldsymbol{e}_z + \eta(t, z)\boldsymbol{e}_r(\theta); \tag{A.1}$$

we recall that

$$\boldsymbol{e}_z = (0, 0, 1), \quad \boldsymbol{e}_r(\theta) = (\cos\theta, \sin\theta, 0), \quad \boldsymbol{e}_\theta(\theta) = \boldsymbol{e}_z \times \boldsymbol{e}_r = (-\sin\theta, \cos\theta, 0) \tag{A.2}$$

where $\theta \in [0, 2\pi]$ is the phase angle around the vessel. We have that the local tangent to the fluid-structure interface profile is given by:

$$\boldsymbol{t}(t, \theta, z) = \left|\frac{\partial p}{\partial z}\right|^{-1} \left(\frac{\partial \boldsymbol{p}}{\partial z}\right) = \left[1 + \left(\frac{\partial \eta}{\partial z}\right)^2\right]^{-1/2} \left(\boldsymbol{e}_z + \frac{\partial \eta}{\partial z}\boldsymbol{e}_r(\theta)\right).$$

This relation is consistent with the expression of the local outward normal to the fluid-structure interface, given in (1.6) by:

$$\boldsymbol{n}_s(t, \theta, z) = \left[1 + \left(\frac{\partial \eta}{\partial z}\right)^2\right]^{-1/2} \left(-\frac{\partial \eta}{\partial z}\boldsymbol{e}_z + \boldsymbol{e}_r(\theta)\right).$$

Let us consider on the vessel wall the three independent variables s, θ, l: $\theta \in [0, 2\pi]$ is the usual circumferential variable, l is the arc-length on the vessel wall profile, given by:

$$l(z) = \int_0^z \left[1 + \left(\frac{\partial \eta}{\partial z}\right)^2\right]^{1/2} dz\,, \qquad z \in [0, L]$$

while $s \in [0, k(t,z)]$ is the position along the local normal $\boldsymbol{n}_s$ to the vessel wall surface. Here $k = k(t,z)$ is the thickness of the vessel wall. The position of a general point Q in the wall is given by (see Figure 3):

$$\boldsymbol{w}(s, \theta, l) = Q - 0 = z\boldsymbol{e}_z + \eta \boldsymbol{e}_r(\theta) + s\boldsymbol{n}_s(t, \theta, z) \tag{A.3}$$

The derivatives of the position vector (A.3) with respect to the local variables s, θ, l are given at time t by:

$$\begin{aligned} a_1 &= \frac{\partial \boldsymbol{w}}{\partial s} = \boldsymbol{n}_s(t, \theta, z) \\ a_2 &= \frac{\partial \boldsymbol{w}}{\partial \theta} = (\eta + s\cos\psi)\boldsymbol{e}_\theta(\theta) \\ a_3 &= \frac{\partial \boldsymbol{w}}{\partial l} = \boldsymbol{t}(t, \theta, z) = (1 + s\chi(t,z))\boldsymbol{t}(t, \theta, z) \end{aligned}$$

where we posed:

$$\cos\psi = \left[1 + \left(\frac{\partial \eta}{\partial z}\right)^2\right]^{-1/2}, \qquad \chi(t,z) = -\frac{\partial^2 \eta}{\partial z^2}\left[1 + \left(\frac{\partial \eta}{\partial z}\right)^2\right]^{-3/2}. \tag{A.4}$$

Remark that $\chi(t,z)$ is the curvature of the line described by the point p introduced in (A.1) as z varies at fixed t while the quantity $\eta + s\cos\psi$ represents the radial distance of the point Q determined by the vector position (A.3) from the centerline of the vessel.

The metric induced by $\boldsymbol{w}$ is orthogonal and given in covariant form by:

$$\underline{G} = g_{ij} = a_i \cdot a_{j\,i,j\in\{1,2,3\}} = \begin{bmatrix} h_s^2 & 0 & 0 \\ 0 & h_\theta^2 & 0 \\ 0 & 0 & h_l^2 \end{bmatrix} \tag{A.5}$$

where:

$$h_s = 1, \quad h_\theta = r = \eta + s\cos\psi, \quad h_l = 1 + s\chi(t,z)\,. \tag{A.6}$$

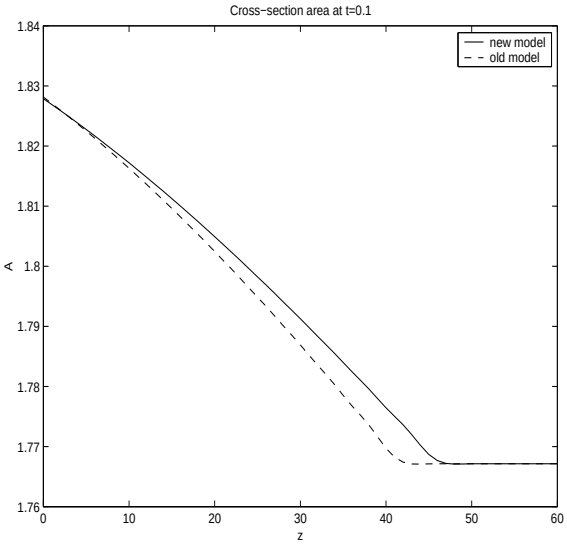

(a) Cross-section area at $t = 0.1$ sec

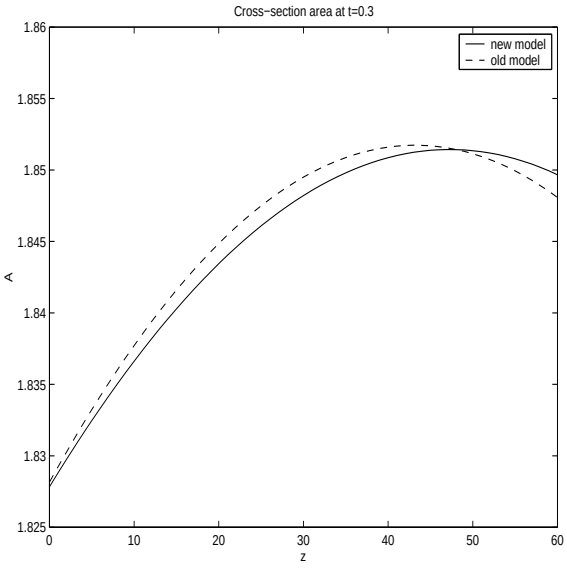

(b) Cross-section area at $t = 0.3$ sec

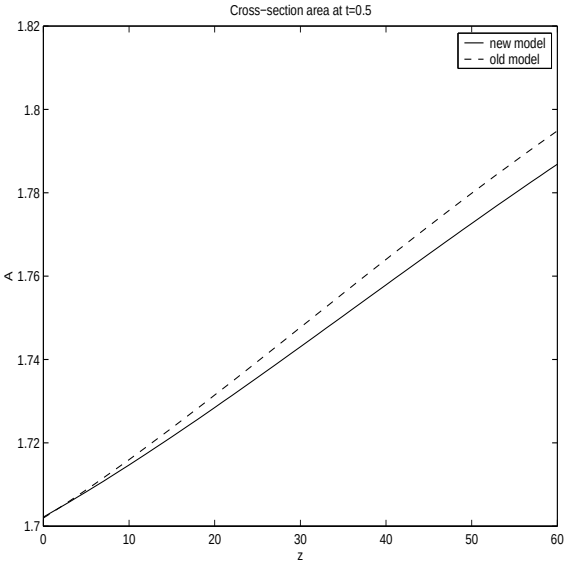

(c) Cross-section area at $t = 0.5$ sec

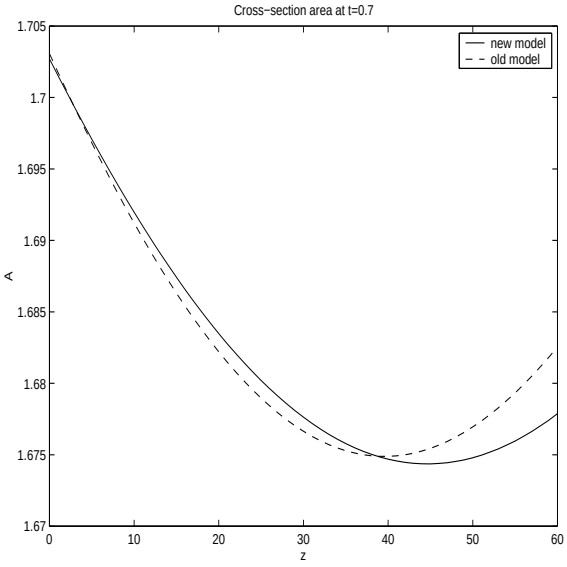

(d) Cross-section area at $t = 0.7$ sec

Figure 4: **Cross-section area. Comparison between old model (dashed line) and new model (solid line).**

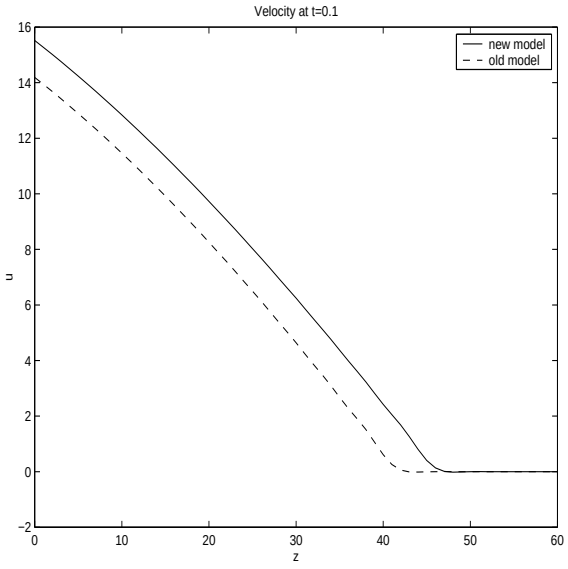

(a) Flux at $t = 0.1$ sec

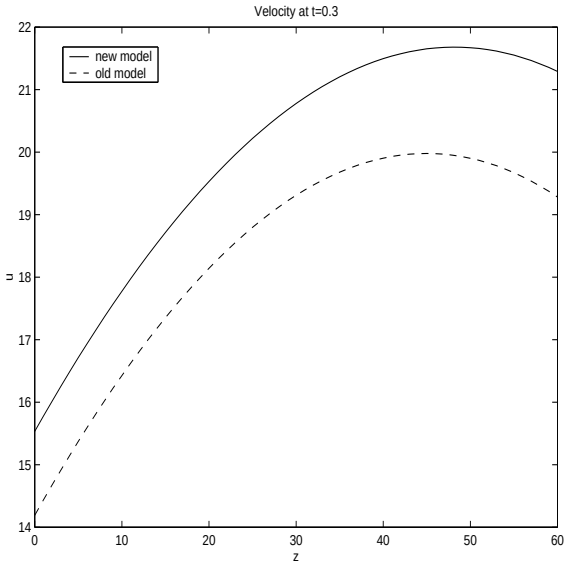

(b) Flux at $t = 0.3$ sec

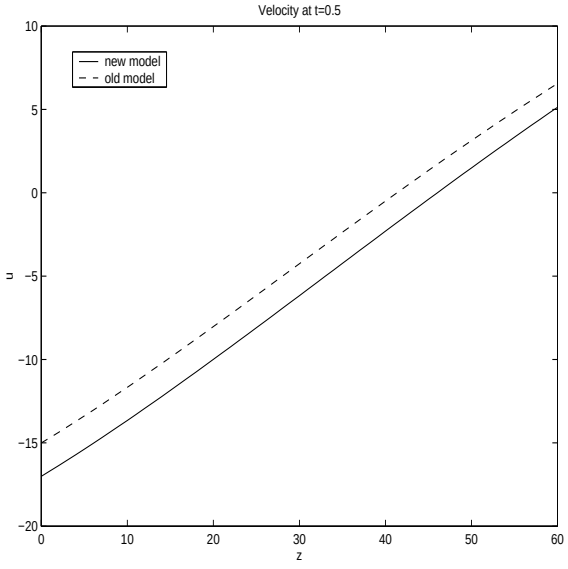

(c) Flux at $t = 0.5$ sec

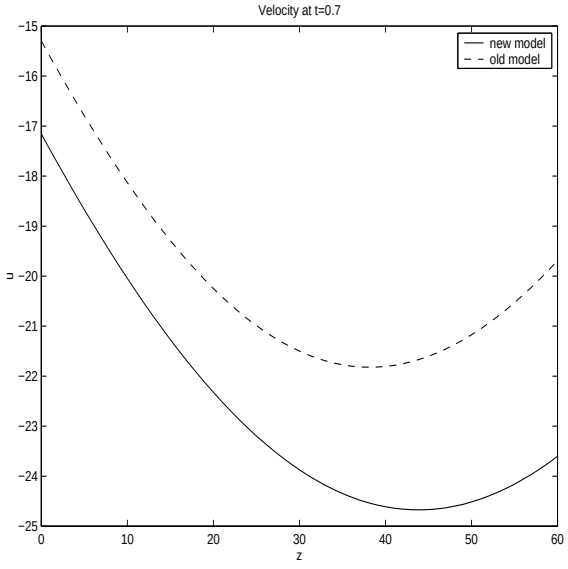

(d) Flux at $t = 0.7$ sec

Figure 5: **Velocity. Comparison between old model (dashed line) and new model (solid line).**

Acknowledgments

The first author acknowledges support by Progetto GNAMPA 2005 *Analisi Asintotica Per Sistemi Iperbolici Nonlineari*. The second author acknowledges the support of the Politecnico di Milano through the CIRIC grant. The third author acknowledges the support of the European Union through the RTN project HaeModel and of the Italian MIUR under project COFIN 2005.

Finally, the authors wish to thank Prof. Alessandro Veneziani for his interest in the present work and his suggestions.

References

[1] R.Aris, *Vectors, tensors and the basic equations of fluid mechanics*, Prentice-Hall, 1962

[2] S.Čanić, E.H.Kim, *Mathematical analysis of the quasilinear effects in a hyperbolic model blood flow through compliant axi-symmetric vessels*, Math.Meth.Appl.Sci. **26** (2003), 1161–1186

[3] S.Čanić, D.Lamponi, A.Mikelić, J. Tambaća, *Self-consistent effective equations modelling blood flow in medium-to large compliant arteries*, Multiscale Model. Simul. **3** (2005), no. 3, 559–596

[4] C.M.Dafermos, *Hyperbolic Conservation Laws in Continuum Physics* (1^{st} Edition), Grundlehren der Mathematischen Wissenschaften **325** (2000) Springer Verlag

[5] A.Di Carlo, P.Nardinocchi, G.Pontrelli, L.Teresi, *A heterogeneous approach for modelling blood flow in an arterial segment*, in Simulation in Biomedicine V (eds. Z. M. Arnez, C.A. Brebbia, F. Solina & V. Stankovski), WIT Press, pp. 69–78, 2003

[6] S.Ferrari, F.Saleri, *A new two-dimensional shallow water model including pressure effects and slow varying bottom topography*, ESAIM: M2AN, **38**, no.2, (2004), 211–234

[7] S.Ferrari, *Convergence analysis of a space-time approximation to a two-dimensional system of shallow water equations*, Applicable Analysis, **83**, no.8, (2004), 757–785

[8] L.Formaggia, J.F.Gerbeau, F.Nobile, A.Quarteroni, *On the coupling of 3D and 1D Navier-Stokes equations for flow problems in compliant vessels*, Comp.Methods in Appl.Mech.Engng.,**191**, (2001), 561–582

[9] L.Formaggia, F.Nobile, A.Quarteroni, A.Veneziani, *Multiscale modelling of the circulatory system: a preliminary analysis*, Comp. Vis. Science, **2** (2000), 163–197

[10] L.Formaggia, A.Veneziani, *Geometrical Multiscale Models for the Cardiovascular System*, in Blood Flow Modelling and Diagnostics, (ed. T.A. Kowaleski), Institute of Fundamental Technological Research, Warsaw, (2005), 309-360.

[11] Y.C.Fung, *Foundations of solid mechanics*, 1972, Prentice-Hall Inc., Canada

[12] Y.C.Fung, K.Fronek, P.Patitucci, *Pseudoelasticity of arteries and the choice of its mathematical expression*, Amer. Physiology Soc.(1979), 620–631

[13] J.-F.Gerbeau, B.Perthame, *Derivation of viscous Saint-Venant system for laminar shallow water; numerical validation*, Discrete Contin. Dyn. Syst. Ser. B **1** (2001), 89–102

[14] A.Quarteroni, L. Formaggia, *Mathematical modelling and numerical simulation of the cardiovascular system*, in Handbook of numerical analysis, Vol. XII (2004), North Holland, Amsterdam, 3–127

[15] S.J. Sherwin, V.Franke, J.Peiró and K.Parker, *One dimensional modelling of a vascular network in space-time variables*, J.Eng.Math, **47** (2003), 217–250

[16] N.P. Smith, A.J. Pullan and P.J. Hunter, *An anatomically based model of transient coronary blood flow in the heart*, SIAM J. Appl. Math.,**62** (2002), 990-1018.

[17] T.-T. Li, *Global classical solutions for quasilinear hyperbolic systems*, Research in Applied Mathematics, (eds P.G. Ciarlet, J-L. Lions). Wiley, New York, 1994

[18] T.-T. Li, B.Rao, Y.Jin, *Semi-global C^1 solution and exact boundary controllability for reducible quasilinear hyperbolic systems*, M2AN, **34**, no.2, (2000), 399-408

[19] T.Pedley, *The fluid mechanics of large blood vessels*, Cambridge University Press, Cambridge, 1980.